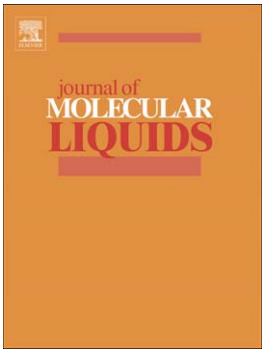

Thermal properties, antimicrobial activity and DNA binding of Ni(II) complexes of azo dye compounds

A.Z. El-Sonbati, M.A. Diab, Sh.M. Morgan

PII: S0167-7322(16)32966-X
DOI: doi:10.1016/j.molliq.2016.11.047
Reference: MOLLIQ 6594

To appear in: *Journal of Molecular Liquids*

Received date: 30 September 2016
Revised date: 14 November 2016
Accepted date: 15 November 2016

Please cite this article as: A.Z. El-Sonbati, M.A. Diab, Sh.M. Morgan, Thermal properties, antimicrobial activity and DNA binding of Ni(II) complexes of azo dye compounds, *Journal of Molecular Liquids* (2016), doi:10.1016/j.molliq.2016.11.047

Thermal properties, antimicrobial activity and DNA binding of Ni(II) complexes of azo dye compounds

A.Z. El-Sonbati [a], M.A. Diab [a], Sh.M. Morgan [b,*]

[a] Chemistry Department, Faculty of Science, Damietta University, Damietta, Egypt

[b] Environmental Monitoring Laboratory, Ministry of Health, Port Said, Egypt

Abstract

A novel series of nickel(II) azo dye complexes of 5-(4-methoxyphenylazo)-2-thioxo-4-thiazolidinone (HL_1), 5-(4-methylphenylazo)-2-thioxo-4-thiazolidinone (HL_2), 5-(phenylazo)-2-thioxo-4-thiazolidinone (HL_3) and 5-(4-nitrophenylazo) -2-thioxo-4-thiazolidinone (HL_4) were prepared and characterized elemental analyses, IR, UV-Visible spectra, X-ray diffraction analysis and mass spectra as well as thermogravimetric analysis (TGA). The magnetic measurements of Ni(II) complexes **(1-4)** lie in 3.05-3.20 BM., as anticipated for octahedral geometry. Quantum chemical parameters and molecular structures of the complexes were theoretically computed and the results were studied. IR spectra show that HL_n ligands (n = 1-4) act a monobasic bidentate ligands by coordinating *via* the oxygen atom of the deprotonated -OH group moiety and nitrogen atom of azo group. The interaction between Ni(II) complexes and calf thymus DNA (CT-DNA) shows hyperchromism effect coupled with obvious bathochromic shift. The value of binding constant (K_b) obtained from the absorption spectral technique for Ni(II) complexes (**1-4**) was calculated and found to be 1.20 x 10^5 , 1.17 x 10^5 , 7.22 x 10^4 and 6.65 x 10^4 M^{-1}, respectively. The antimicrobial activities of Ni(II) complexes **(1-4)** were investigated. It was found that the Ni(II) complexes have low antibacterial activity against *Klebsiella pneumoniae*. Complex **(1)** has antifungal activity against *Penicillium italicum*. All the Ni(II) complexes have more antibacterial activity than the penicillin against *Klebsiella pneumoniae*. The thermodynamic parameters were calculated using Coats–Redfern and Horowitz–Metzger methods. From the values of the thermal activation energy for decomposition (E_a) of Ni(II) complexes **(1-4)**, it was found that the E_a value for the complex **(4)** is higher compared to the other complexes. The positive value of Gibbs free energy change of the decomposition (ΔG^*) for the Ni(II) complexes is non-spontaneous processes.

Keywords: Ni(II) complexes; Calf thymus DNA; X-ray diffraction analysis; Thermal analysis; Thermodynamic parameters; Antimicrobial activity.

*Corresponding author: E-mail: shimaa_mohamad2010@yahoo.com (Sh.M. Morgan).

1. Introduction

Coordination chemistry is basically the chemistry of the electron accepting behavior of metal ions surrounded by ligands. The wide range of color exhibited by coordination compounds and their structures which are signs of the coordination number of the metal ion and the ligational behavior of the complexing agents, make their investigation very challenging and at the same time interesting [1-3]. The azo compounds are characterized by the presence of one or more azo groups. The formation of azo compounds usually involves the reaction between a diazo species and a coupling agent.

Rhodanine azo dye compounds are the most widely used class of coloring materials because of the huge demand in the various fields of technology and science [3,4]. A lot of investigation has been carried out in recent years on the synthesis and spectral the characteristics of this group of dyes [2,5]. Besides, the azo compounds are known to be involved in some biological reactions such as inhibition of DNA and biological activity against bacteria and fungi [2,4,6]. The rhodanine compounds were effectives against Gram positive and Gram negative bacteria [4] that can be used in a wide range of application. Advancement of metal complexes as artificial nucleases was an area of interest. Various reports have additionally pointed out several cases of complexes due to their vast potential utilities through their interactions against bacteria and fungi activity [4,7]. Chemical properties of rhodanine compounds are of interest due to coordination capacity and their use as metal extracting agents and as analytical reagents [8,9].

Rhodanine and its derivatives are quite interesting which have gained special attention in the last decade, not only because of the structural chemistry and their importance in medical chemistry. Rhodanine derivatives have broad spectra of pharmacological activities and these compounds were used in the pharmaceutical industry and applications in many vital areas. Rhodanine and its derivatives are known to possess biological activities [10,11] such as potential antimycobacterial [12], antifungal [13], antibacterial [14], antiviral [15] and antidiabetic mechanism [16]. The studies revealed that such type of molecule exhibit as inhibitors of numerous targets such as histidine decarboxylase [17], β-lactamase [18], JNK Stimulatory Phosphatase-1 (JSP-1) [19] in addition to rhodanine derivatives were also reported as hepatitis C virus (HCV) protease inhibitor [20,21].

Recently in our laboratory, numerous azo/hydrazone complexes of rhodanine and its derivatives have been reported [2,7]. In this paper, we investigate the molecular structures, elemental analyses, IR spectra, spectral studies, molar conductance, magnetic measurements, mass spectra, X-ray diffraction analysis, thermal study and thermodynamics parameters of nickel(II) azo dye complexes with 5-(4-methoxyphenylazo)-2-thioxo-4-thiazolidinone (HL_1), 5-(4-methylphenylazo)-2-thioxo-4-thiazolidinone (HL_2), 5-(phenylazo)-2-thioxo-4-thiazolidinone (HL_3) and 5-(4-nitrophenylazo) -2-thioxo-4-thiazolidinone (HL_4). The molecular structures of Ni(II) complexes are discussed and quantum chemical parameters are calculated. Ni(II) complexes are screened for their antimicrobial activity against bacteria and fungi species. The calf thymus DNA (CT-DNA) binding activity of Ni(II) complexes are studied by absorption spectra.

2. Experimental

2.1. Materials

All the chemicals used were of British Drug House (BDH) quality and were used without any further purification. The calf thymus DNA (CT-DNA) was acquired from SRL (India). Double distilled water was utilized to prepare all the buffer solutions.

2.2. Preparation of the ligands (HL_n)

HL_n ligands were prepared according to the method [1-4]. Azo dye compounds are prepared by an aqueous diazotization and coupling procedure, which lead to a pure product in high yield and in a physical form suitable for application [22,23]. The purity of ligands was checked by Thin-layer chromatography (TLC). TLC analysis was performed on silica gel utilizing the dissolvable framework benzene/acetone (1:2) as solvent.

2.3. Preparation of Ni(II) complexes

The Ni(II) complexes were prepared by refluxing a hot ethanolic solution containing azo dye rhodanine derivatives was mixed with a hot ethanolic solution of $Ni(CH_3COO)_2.4H_2O$ (1 mmol). The mixture was then refluxed on a water bath for ~ 6-8 hrs and allowed to cool then the solid complexes are separated, filtered, washed a few with ethanol, diethyl ether and finally dried in a vacuum desiccators over

anhydrous $CaCl_2$. The yields of the final products were 78-88%. Table 1 shows the analytical data of Ni(II) complexes (Fig. 1).

2.4. Biological activity investigation

For this examination was applied the method of agar well diffusion [4]. The antibacterial activities of the investigated compounds were tested against two local Gram positive bacterial types (*Staphylococcus aureus* and *Bacillus cereus)* and two local Gram negative types (*Escherichia coli* and *Klebsiella pneumoniae*) on nutrient agar medium. As well, the antifungal activities were tested against four local fungal types (*Penicillium italicum*, *Alternaria alternata*, *Aspergillus niger* and *Fusarium oxysporium*) on DOX agar medium. The concentrations of every solution of compound were 50, 100 and 150 µg/mL in dimethyl formamide (DMF). Utilizing a sterile cork borer (10 mm diameter), wells was made in medium of agar plates previously seeded with the test microorganism. 200 µL of every compound was applied in every well. The agar plates were kept at 4 °C for at least 30 min to allow the diffusion of the compound to agar medium. The plates were then incubated at 37 °C or 30 °C for bacteria and fungi, respectively. The diameters of inhibition zone were specified after 24 h and 7 days for days for bacteria and fungi, respectively, taking the consideration of the control values (DMF). Penicillin and miconazole were used as standard drugs against bacteria and fungi, respectively.

2.5. DNA binding experiments

The binding properties of Ni(II) complexes to CT-DNA are studied using electronic absorption spectroscopy. The stock solution of CT-DNA is prepared in 5 mM Tris-HCl / 50 mM NaCl buffer (pH=7.2), which a ratio of UV absorbance at 260 and 280 nm (A_{260}/A_{280}) of calculated 1.8 -1.9, indicating that the DNA is sufficiently free of protein [24], and the concentration is determined by UV absorbance at 260 nm (ε = 6600 M^{-1} cm^{-1}) [25]. Electronic absorption spectra are carried out using 1 cm quartz cuvette at room temperature by fixing the concentration of complex (1.00×10^{-3} mol L^{-1}), while progressively increasing the concentration of calf thymus DNA (CT-DNA) (0.00 to 1.30×10^{-4} mol L^{-1}). An equivalent amount of CT-DNA is added to both the solutions of compound and the references buffer solution to eliminate the absorbance of CT-DNA itself. The intrinsic binding constant K_b of the compound with CT-DNA is determined using the following equation (1) [24]:

$$[DNA] / (\epsilon_a - \epsilon_f) = [DNA] / (\epsilon_b - \epsilon_f) + 1 / K_b(\epsilon_a - \epsilon_f) \quad (1)$$

where [DNA] is the concentration of CT-DNA in base pairs, ϵ_a is the molar extinction coefficient observed for the A_{obs}/[compound] at the given DNA concentration, ϵ_f is the molar extinction coefficient of the free compound in solution and ϵ_b is the molar extinction coefficient of the compound when fully bond to DNA. In plots of [DNA]/(ϵ_a–ϵ_f) versus [DNA] and K_b is given by the ratio of the slope to the intercept.

2.6. Measurements

Elemental microanalyses of the complexes for C, H, N and S were analyzed on Automatic Analyzer CHNS Vario ELIII, Germany. Infrared spectra were recorded using a Perkin-Elmer 1340 spectrophotometer as KBr discs. Mass spectra were recorded using MS-5988 GS-MS Hewlett-Packard by the EI technique at 70 eV. X-ray diffraction analysis of complexes was recorded on X-ray diffractometer analysis in the range of diffraction angle $2\theta^o$ = 4–80^o. This analysis was done utilizing CuKα radiation (λ = 1.540598 Å). The tube current and the applied voltage are 30 mA and 40 kV, respectively. Ultraviolet-visible spectra of the complexes were registered in nujol mulls using a Unicom SP 8800 spectrophotometer. The magnetic moment of the complexes was determined using the Gouy`s method at room temperature. Mercury(II) (tetrathiocyanato)cobalt(II), [Hg{Co(SCN)$_4$}], was utilized for the calibration of the Gouy tubes. Corrections of diamagnetic were calculated from the values given by Selwood [26] and Pascal's constants. Magnetic moments were computed utilizing the equation, $\mu_{eff.} = 2.84\ [Tc_M^{coor.}]^{1/2}$. The thermal studies were computed on Simultaneous Thermal Analyzer (STA) 6000 system using thermogravimetric analysis method. Thermal properties of the samples were anatomized at the heating rate of 10 ^{o}C/min under dynamic nitrogen atmosphere in the temperature range from 30 to 800 °C. Molecular structures of the compounds were optimized by HF technique with 3-21G basis set. The molecules were built with the Perkin Elmer ChemBio Draw and optimized utilizing Perkin Elmer ChemBio3D software [7].

2.7. Statistical Analysis

Data were statistically analysed for variance and the least significant difference (LSD) at 0.05 level using one-way analysis of variance (ANOVA) were carried out by SPSS software version 17.

3. Results and discussion

3.1. The structure and molecular geometry optimization of Ni(II) complexes

All complexes were found to form readily from the reaction mixture of the appropriate nickel(II) acetate and the ligand (HL_n) in hot ethanolic. The analytical data of the experimental and theoretical data of (%C, %H, %N, %S and %Ni) are in a good agreement with suggests the formulation $[Ni(L_n)(CH_3COO)(OH_2)_2].nH_2O$ as shown in Table 1 and Fig. 1. Nickel(II) complexes are stable with highly melting points (> 300 ^oC), insoluble in H_2O and soluble in warm DMSO and DMF. The molar conductance values of all complexes in 10^{-3} M solution in DMF are found to be less than 20 Ω^{-1} mol^{-1} cm^2, showing that they are non-electrolytes indicating its non-electrolytic nature [7] which indicate that the anion and the ligand are coordinated to the central nickel(II). The magnetic moment of Ni(II) complexes was estimated at room temperature and has a paramagnetic nature octahedral geometry.

Molecular modeling and quantum chemical parameters of Ni(II) complexes (**1-4**) were calculated theoretically and listed in Table 2 (Fig. S1). Also, corresponding geometric parameters bond lengths and bond angles of Ni(II) complexes (**1-4**) are listed in Tables S1-S4. The quantum chemical parameters were calculated and the calculated parameters are identified as follows [5]:

- The highest occupied molecular orbital energy (E_{HOMO})
- The lowest unoccupied molecular orbital energy (E_{LUMO})
- The HOMO–LUMO energy gap (the difference between HOMO and LUMO energy levels) (ΔE)
- Absolute electronegativities (χ)
- Chemical potential (Pi)
- Absolute hardness (η)
- Absolute softness (σ)
- Global electrophilicity (ω)
- Global softness (S)
- Electronic charge (ΔN_{max})

Figure 2 shows the HOMO and LUMO orbital's for Ni(II) complexes **(1-4)**. As indicated the frontier molecular orbital theory, FMO, the chemical reactivity is a function of interaction between HOMO and LUMO levels of the reacting species [5,7]. The E_{HOMO} frequently connected with the electron donating ability of the molecule to donate electrons to appropriated acceptor molecules with low-energy, empty molecular orbital [5]. Likewise, E_{LUMO} indicates the ability of the molecule to

accept electrons. The higher is the value of E_{HOMO} of the complexes; the easer is its offering electrons. The value of low energy gap performs to soft molecules which is more reactivity and high flexibility. The calculation of absolute softness (σ) parameter is useful to recognize the molecular stability and reactivity. It was found that the stability of the Ni(II) complexes increase with the order: complex **(4)** < complex **(3)** < complex **(2)** < complex **(1)** related to ΔE values (Table 2), as expected electron donating group has lower energy gap and higher stability compared with electron withdrawing group as shown in Fig. 3.

3.2. Structure of ligands (HL_n)

Classic-azo-enol dyes are prepared by an aqueous diazotization and coupling procedure, which lead to a pure product in high yield and in a physical form suitable for application [27-29]. The azo dyes prepared in this study may exist in tautomeric forms as shown in azo-keto (Fig. 1A), azo-enol (Fig. 1B) and keto-hydrazone (Fig. 1C).

El-Sonbati et al. [27,28] found that three types of hydrogen bonds may exist in equilibrium with each other. The hydrogen bond in this case is of intramolecular type either with (B) or (C) and intermolecular hydrogen bonding can form cyclic dimmer through the (E) and/or (F) as shown in Fig. 1. The azo dye ligands have been demonstrated conclusively from a series of investigations using a variety techniques, such as IR spectra, the HL_n ligands exist exclusively in azo-enol form in solution [1A↔1B] (Fig. 1) [2]. The six-membered intramolecular hydrogen bonding ring is possible in the azo-enol tautomer (Fig. 1).

The infrared spectra are consistent with the formation of HL_n ligands. The vibrational assignments were aided by comparison with the vibrational frequencies of the related compounds as *p*-derivative aniline and 2-thioxo-4-thiazolidinone. The fundamental stretching mode of the azo dye moiety, υ(N=N), is readily assigned by comparison with the infrared spectra of derivatives of aniline and ligands (HL_n). The absorption bands due to amino (NH_2) of stretching vibration disappeared and instead a new band assigned to azo dye υ(N=N) linkage appeared at ~ 1540 cm^{-1} [7] (Fig. 1).

The ligands under investigation are capable of exhibiting azo-enol (Fig. 1B) and keto-hydrazone (Fig. 1C) tautomerism. It has been reported that azo dye rhodanine derivatives exist predominantly in the azo-enol form [30].

3.3. Structure of the metal chelates

- Infrared spectra of the ligand (HL_n) exhibited a broad medium intensity band ranging ~ 3340-2980 cm^{-1} and centered at ~3210 cm^{-1}, which could be assigned to hydrogen bonded enolic υ(C–O) stretching vibration [31]. A strong band at ~1275-1265 could be attributed to υ(C–O) vibration of C–O group [32]. A medium intensity band at ~ 1540 cm^{-1} was assignable to the stretching vibration of N=N group [2,7].
- In all complexes, the hydrogen bonded enolic –OH band disappeared, attributed to the deprotonation and formation of metal-oxygen bond. This is supported by the shifting of υ(C–O) towards higher frequencies as compared to the free ligands due to the conversion of hydrogen bonded structure into a covalent metal bonded structure [2].
- The N=N stretching frequency of the azo group is shifted to lower frequencies by ~25-30 cm^{-1} attributed to the involvement of one of the azo nitrogen atom in coordination with metal ion [7]. This lowering of frequency can be explained by the transfer of electrons from the nitrogen atom to the metal ion due to coordination.
- From infrared spectra of the metal complexes show several non ligand bands of low intensity appearing in the region 515-540 and 445-460 cm^{-1} can be assigned to υ(M–O) and υ(M–N), respectively, [2,7].
- Absence of υ(M–S) band in the far IR spectra gives added evidence for the non participation of ring sulfur atom in bond formation.
- Ni(II) complexes exhibits distinct bands at ~1590 and ~1450 cm^{-1} due to the asymmetric and symmetric modes of vibration characteristic of CH_3COO, respectively, and with $\Delta\upsilon$ = 140 cm^{-1} which is consistent with the bidentate nature of the acetate group [33], this is further supported by the appearance of δ(O–C–O) wagging modes of acetate around 680 and 620 cm^{-1} [34]. A broad band around 3410 cm^{-1} is attributed to υ(O–H) aqua of coordinated water. On complex formation, the new peak observed at ~565 may be assigned to chelate ring deformation [35].
- The appearance of a new bands around 2450 cm^{-1} in the prepared Ni(II) complexes may be taken as a strong evidence for the presence of coordinated water and also suggest that H-bonding interaction exists between the water molecule and the carboxylate oxygen of acetate group. Such region, however, is not initially present in the free ligands. This is confirmed by the elemental analysis of these complexes (Table 1).

- Molecular structure of all complexes could be suggested based on: (i) the presence of one anion, (ii) the disappearance of C=O, (iii) the coordination of azo group and (iv) the coordination of water molecules.

Based on these information's obtained from the spectra and other investigations, the bonding in Ni(II) complexes may be represented as shown in Fig. 1.

3.4. Magnetic moment and spectral studies

Azo dye ligands (HL_n) react with freshly prepared solutions of nickel(II) acetate to give complexes of the type $[Ni(L_n)(CH_3COO)(OH_2)_2].nH_2O$. The magnetic measurements of Ni(II) complexes **(1-4)** lie in the range of 3.05-3.20 BM., as expected for octahedral geometry around the metal ions. The reflectance spectra of the Ni(II) complexes are characterized by three main bands in the regions $^3A_{2g} \rightarrow {}^3T_{2g}(\upsilon_1)$ (12770-13280 cm^{-1}), $^3A_{2g} \rightarrow {}^3T_{1g}(\upsilon_2)$ (14640-18580 cm^{-1}) and $^3A_{2g} \rightarrow {}^3T_{1g}(P)(\upsilon_3)$ (24210-27625 cm^{-1}) transition in an idealized O_h-symmetry [36]. The computed values of υ_2/υ_1 are proportionate with an octahedral configuration proposing strong T_{1g}-term interactions of nickel(II) complexes [37]. The low values of υ_2/υ_1 are due to the strong interaction between $^3T_{1g}(P)$ and $^3T_{1g}(F)$ states. The value of B are lower than the free ion, there is due to orbital overlap and delocalization of d-orbital. Ligand field stabilization energy (LFSE kcal mol^{-1}) has been calculated [38]. The energies of these bands were used to calculate the electronic spectral parameters of the nickel(II) complexes according to Lever's method [38] and the electronic parameters are listed in Table 3. The Dq/B value was taken to measure the extent of distortion in this symmetry The covalency factor (β) is less than unity, this can be assigned upon the metal-ligand bonds have a considerable of covalent character. The percentage lowering of energy in free gaseous ion (β^o % = 41.6 – 87.4%) are calculated (Table 3). The reduction of the Racah parameter (B) can be calculated from the following equation [39]:

$$B_{complex} = (2\upsilon_1^2 + \upsilon_2^2 - 3\upsilon_1\upsilon_2)(15\upsilon_2 - 27\,\upsilon_1) \quad (2)$$

The covalency factor was calculated from the following equation:

$$\beta = B/B` \text{ (B` is the free nickel ion = 1038 } cm^{-1}\text{).} \quad (3)$$

The relation between Dq and Hammett's substituent coefficients (σ^R) is shown in Fig. S2, it is clear that the value of Dq increase with decreasing the value of σ^R. The

values of Dq the order of binding complex is as follows: complex **(1)** > complex **(3)** > complex **(4)**.

3.5. Mass spectra

The mass spectrum of $[Ni(L_3)(CH_3COO)(OH_2)_2]H_2O$ **(3)** complex (Scheme 1) exhibits a parent molecular ion peak at m/z 407.69 (1.0%) which is equal to the formula weight of the complex $[NiC_{11}H_{13}N_3O_5S_2]H_2O$. The peak at m/z 338.69 (9%) formed from complex **(3)** through the removal of $3H_2O$ molecules and methyl group (structure **I**). The spectrum shows molecular ion peaks at m/z 262.69 (17%), 99 (28%) and 71 (34%) corresponding to the $[NiC_9H_6N_3OS]$ (structure **II**), $[C_3HNOS]$ (structure **III**) and $[C_2HNS]$ (structure **IV**) fragments, respectively. The information gathered from mass spectrum data of Ni(II) complex **(3)** is good agreement with the proposed molecular formula for this complex.

3.6. X-ray diffraction analysis

The X-ray diffraction, XRD, patterns of Ni(II) complexes (**2-4**) powder forms are shown in Fig. 4. The XRD patterns show a broad peak in the range of $2\theta^o$ = 23- 26^o indicating a completely amorphous structures.

3.7. DNA binding studies

Absorption titration is a standout amongst the most generally utilized methods to study the binding modes and binding extent of compounds to DNA. Absorption titration experiments are performed with fixed concentrations of Ni(II) complexes (**1-4**) (40 μM) while gradually increasing the concentration of calf thymus DNA (CT-DNA) (10 mM). While measuring the absorption spectra, an equivalent value of DNA was added to both the compound solution and the reference solution to eliminate the absorbance of DNA itself. We have determine the intrinsic binding constant to CT-DNA by monitoring the absorption intensity of the charge transfer spectral bands near 427, 425, 428 and 440 nm for Ni(II) complexes (**1-4**), respectively. Absorption spectra of Ni(II) complexes **(1-4)** increase with increasing the volume of CT-DNA are in the range 300-600 nm as shown in Fig. 5 and Fig. S3.

The interaction between Ni(II) complexes **(1-4)** and calf thymus DNA (CT-DNA) has been studied by UV Visible spectroscopy electronic absorption spectra.

After interaction of Ni(II) complexes **(1-4)** and with increasing the amount of calf thymus DNA (CT-DNA), it was found that all the peaks increased gradually and the wavelengths have minor red shift (bathochromic shift) of 2 nm. The binding involves a typical intercalative mode, a hyperchromism effect coupled with obvious bathochromic shift for the distinguishing peaks of the small molecules will be found due to the strong stacking between the chromophore and the base pairs of DNA [40]. Therefore, based on this viewpoint, the interaction between Ni(II) complexes (**1-4**) and calf thymus DNA could be noncovalent intercalative binding.

Plot of $[DNA]/(\varepsilon_a - \varepsilon_f)$ as function of DNA concentration as determined from the absorption spectral data was shown in Fig. 6 and Fig. S4. The value of binding constant (K_b) obtained from the absorption spectral technique for Ni(II) complexes (**1-4**) was calculated and found to be 1.20 x 10^5, 1.17 x 10^5, 7.22 x 10^4 and 6.65 x 10^4 M^{-1}, respectively. Binding constant values are related to the nature of the substituent as they increase according to the following order *p*-(OCH_3 > CH_3 > H > NO_2). That is attributed to the *p*-substituent's of azo moiety as electron donating group which increases the electron density in the benzene ring by its high electron donating mesomeric or inductive effects; there by stronger hydrogen bond is formed. The relation between binding constant (K_b) and Hammett's substituent coefficients (σ^R) is shown in Fig. 7, it is clear that the value of K_b increase with decreasing the value of σ^R, is due to exists donating group. From these results it may be generalized that the more binding complex has more high value of binding constant (K_b) so that from the values of K_b the order of binding complex is as follows: Ni(II) complex **(1)** > Ni(II) complex **(2)** > Ni(II) complex **(3)** > Ni(II) complex **(4)**.

3.8. Thermal analysis of Ni(II) complexes

Thermal analysis is useful in determining the water molecules content in the complexes and their thermal stability. The thermal stability properties were evaluated by TG method whose results revealed good thermal stability for all the complexes. In general, it was observed that the sequence of degradation that takes place in these complexes starts with dehydration of lattice water molecules followed by the release of coordination water and then fragments of a part of the ligand. Thermogravimetric analysis (TGA) curves of Ni(II) complexes **(1-4)** are displayed in Fig. 10 and the thermal decomposition results are listed in Table 4. The first stage of decomposition in the range ~35-110 ºC for Ni(II) complexes can be attributed to loss of lattice water molecule [7] (Fig. 8). The second stage of decomposition corresponds to the loss of

coordinated water molecule and coordinated acetate group and decomposition of a part of the ligand. The third stage is attributed to loss of a part of the ligand. The remaining final product is nickel oxide residue with contaminated carbon atoms (Table 4).

In conclusion, the thermal studies were significantly helpful for the elucidation of crystallisation of water, degradation temperature and thermal stability of complexes for every decomposition step in thermal analysis processes.

3.9. Thermodynamic studies

The thermodynamic parameters are calculated using the Coats-Redfern and Horowitz-Metzger methods [41,42]. The thermal activation energy for decomposition (E_a) and entropy (ΔS^*) were calculated. The enthalpy (ΔH^*) and Gibbs free energy change of the decomposition (ΔG^*) were calculated from $\Delta H^* = E_a - RT$ and $\Delta G^* = \Delta H^* - T\,\Delta S^*$, respectively.

The thermodynamic data obtained with the two methods for Ni(II) complexes **(1-4)** are listed in Table 5 and Figures 9 and 10. The thermodynamic results obtained from the Coats-Redfern and Horowitz-Metzger methods are comparable and can be considered in good agreement with each other [43]. From the values of the thermal activation energy for decomposition (E_a) of Ni(II) complexes **(1-4)**, it was found that the E_a value for the complex **(4)** is higher compared to the other complexes.

The entropy reflects the thermal stability of the compounds. The entropy is found to be negative values in the Ni(II) complexes **(1-4)** which indicates more ordered activated complex than the reactants or the reaction is slow [7,44]. The positive value of ΔG^* for the Ni(II) complexes **(1-4)** is non-spontaneous processes. Also, the values of ΔG^* increases significantly for the subsequent decomposition stages of a given complex. This is due to increasing the values of T ΔS^* significantly from one stage to another which overrides the values of ΔH^* [45].

3.10. Antimicrobial studies

The antimicrobial activity was assessed based on the size of inhibition zone around dishes. Antimicrobial activity of rhodanine azo dye derivatives and their metal complexes may be significantly enhanced by the presence of nitrogen, oxygen and sulfur atoms which have chelating properties [2,7]. These properties may be used in metal transport across the bacterial membranes or to append to the bacterial cells at a particular site from which it can meddle with their growth.

Antibacterial and antifungal activities of Ni(II) complexes (**1-4**) were tested against Gram positive bacteria as *Staphylococcus aureus* and *Bacillus cereus* and Gram negative bacteria as *Escherichia coli* and *Klebsiella pneumoniae* and fungi species as *Aspergillus niger, Fusarium oxysporium, Penicillium italicum* and *Alternaria alternata*. The results of the antibacterial activity of Ni(II) complexes **(1-4)** were recorded in Table 6. All the Ni(II) complexes **(1-4)** have low antibacterial activity against *K. pneumoniae* and have no antibacterial activity against *S. aureus* and *B. cereus*. It was found that Ni(II) complexes **(1-4)** have more antibacterial activity than the penicillin against *K. pneumoniae* at all tested concentrations (Fig. 11).

The antifungal activity results of the Ni(II) complexes (**1-4**) were listed in Table 7. It was found that the Ni(II) complexes (**1-4**) have no antifungal activity against *F. oxysporum* and *A. alternata*. While the complexes (**1**) and (**3**) have antifungal activity against *P. italicum* (Fig. 12). The complexes (**3**) and (**4**) have antifungal activity than the other complexes against *A. niger*. The complex **(1)** has more antifungal activity than the miconazole against *P. italicum* at 50 and 100 µg/ml. Our results are similar to Habib et al. [46] who studied the antimicrobial activities of some rhodanine derivatives and they revealed that the most pronounced activity was the antifungal activity against *A. niger* and *Penicillium* sp.

Conclusions

The molecular structures, elemental analyses, IR spectra, spectral studies, molar conductance, magnetic measurements, mass spectra, X-ray diffraction analysis, thermal study and thermodynamics parameters of Ni(II) complexes have been discussed. It was found that the stability of the Ni(II) complexes **(1-4)** increase with the order: complex **(4)** < complex **(3)** < complex **(2)** < complex **(1)** related to ΔE values, as expected electron donating group has lower energy gap and higher stability compared with electron withdrawing group. The values of the thermal activation energies for decomposition (E_a) of complexes $[Ni(L_n)(CH_3COO)(OH_2)_2].nH_2O$ **(1-4)**, are found to be in the rang 38-60 kJ/mol. Ni(II) complexes are screened for their antimicrobial activity against bacteria and fungi species. It was found that Ni(II) complexes **(1-4)** have more antibacterial activity than the penicillin against *Klebsiella pneumoniae*. The tested complex **(1)** has antifungal activity against *Penicillium italicum*.

Acknowledgement

The authors would like to thank Prof. Dr. M.I. Abou-Dobara, Botany Department, Faculty of Science, Damietta University, Egypt for his help during testing antimicrobial activity.

Appendix A: Supplementary material

See the attached file.

References

[1] A.Z. El-Sonbati, M.A. Diab, A.A. El-Bindary, Sh.M. Morgan, Inorg. Chim. Acta 404 (2013) 175–187.

[2] M.A. Diab, A.Z. El-Sonbati, A.A. El-Bindary, G.G. Mohamed, Sh.M. Morgan, Res. Chem. Intermed 41 (2015) 9029–9066.

[3] N.A. El-Ghamaz, A.Z. El-Sonbati, Sh.M. Morgan, J. Mol. Struc. 1027 (2012) 92–98.

[4] M.I. Abou-Dobara, A.Z. El-Sonbati, Sh.M. Morgan, World J. Microbiol. Biotechnol. 29 (2013) 119 -126.

[5] A.Z. El-Sonbati, I.M. El-Deen, M.A. El-Bindary, J. Mol. Liq. 215 (2016) 612–624.

[6] E.R.A. Ferraz, M.D. Grando, D.P. Oliveira, Journal of Hazardous Materials, 192 (2011) 628–633.

[7] A.Z. El-Sonbati, M.A. Diab, A.A. El-Bindary, A.M. Eldesoky, Sh.M. Morgan Spectrochim. Acta A 135 (2015) 774–791.

[8] W.I. Stephen, A. Townshend, Anal. Chim. Acta 33 (1965) 257-265.

[9] G. Galan Alfonso, J.L. Gomez Ariza, Microchem. J. 26 (1981) 574-585.

[10] D. B. J. Boyd, J. Mol. Struc. 401 (1997) 227–234.

[11] N.H. Metwally, M.A. Abdalla, M.A.N. Mosselhi, E.A. El-Desoky, Carbohydr Res 345 (2010) 1135‑1141.

[12] H. Taniyama, B. Yasui, N. Takehara, H. Uchida, Yakugaku Zasshi, 79 (1959) 1465–1468.

[13] M.G. Orchard, J.C. Neuss, C.M.S. Galley, Bioorg. Med. Chem. Lett. 14 (2004) 3975–3978.

[14]T. Tomasic, N. Zidar, M. M. Premru, D. Kikelj, L. P. Masic, Eur. J. Med. Chem. 45 (2010) 1667–1672.

[15] V. Enchev, S. Chorbadjiev, B. Jordanov, Chem. Heterocycl. Compd. 38 (2002) 9–19.

[16] Y. Momose, K. Meguro, H. Ikeda, C. Hatanaka, S. Oi, T. Sohda, Chem. Pharm. Bull. 39 (1991) 1440–1446.

[17] C. A. Free, E. Majchrowich, S. M. Hess, Biochemical Pharmacology, 20 (1971) 1421–1428.

[18] A. Zervosen, W. P. Lu, Z. Chen, R. E. White, T. P. Demuth Jr., J. M. Frere, Antimicrobial Agents and Chemotherapy, 48 (2004) 961–969.

[19] N. S. Cutshall, C. O'Day, M. Prezhdo, Bioorg. Med. Chem. Lett. 15 (2005) 3374–3379.

[20] K. Sudo, Y. Masumoto, M. Matsushima, M. Fujwara, K. Konno, K. Shimotohno, S. Shigerta, T. Yokora, Biochem. Biophys. Res. Comm. 238 (1997) 643–647.

[21] W.T. Sing, C.L. Lee, S.L. Yeo, S.P. Lim, M.M. Sim, Bioorg. Med. Chem. Lett. 11 (2001) 91–94.

[22] R.H. Christie, P.N. Standring, Dyes Pigments 9 (1988) 37.

[23] A.Z. El-Sonbati, M.A. Diab, M.M. El-Halawany, N.E. Salam, Spectrochim. Acta A 77 (2010) 755–766.

[24] A. Wolfe, G.H. Shimer, T. Meehan, Biochemistry 26 (1987) 6392–6396.

[25] M.F. Reichmann, C.A. Rice, C.A. Thomos, P. Doty, J. Am. Chem. Soc. 76 (1954) 3047–3053.

[26] P.W. Selwood, Magnetic Chemistry, Interscience Pub. Inc., New York, 1956.

[27] A.Z. El-Sonbati, A.A.M. Belal, M.S. El-Gharib, Sh.M. Morgan, Spectrochim. Acta Part A 95 (2012) 627–636.

[28] A.Z. El-Sonbati, M.A. Diab, A.A.M. Belal, Sh.M. Morgan, Spectrochim. Acta Part A 99 (2012) 353–360.

[29] R.H. Christie, P.N. Standring, Dyes Pigments 9 (1988) 37.

[30] K. Krishnankutty, P. Sayudevi, M.B. Ummathur, J. Indian Chem. Soc. 84 (2007) 518–523.

[31] E. Huang, Y. Wu. D. Gu,F. Gan, Dyes Pigments 66 (2005) 77-82.

[32] K. Krishnankutty, P. Sayudevi, M.B. Umnathur, J. Indian Chem. Soc., 84 (2007) 337-340.

[33] A. El-Dissouky, A.M. Hindawy, A. Abdel-Salam, Inorg. Chim. Acta, 117 (1986) 109.

[34] E.N. Sakuntula, G. Srivastova, R.C. Mehrotra, Indian J. Chem., 20A, (1981) 243.

[35] A.Z. El-Sonbati, A.M. Hassanein, M.A. Hefni, Spectroscopy Lett., 26, (1993) 1311.

[36] F.A. Cotton and G. Wilkinson, "Advanced Inorganic Chemistry", 2nd. Edit., Wiley Eastern Private Ltd., New Delhi, 1972, p. 869-881.

[37] L. Sacconi, "Transition Metal Chemistry" (Edited by R.L. Carlin), Vol. 4. P. 199. Marced Dekker, New York (1968).

[38] A.P.B. Lever, "Crystal Field Spectra, Inorganic Electronic Spectroscopy", first ed., Elsevier, Amsterdam, 1968.

[39] A.B.P. Lever, J. Chem. Edu., 45 (1968) 711.

[40] Y. Liu, K. Zhang, Y. Wu, J. Zhao, J. Liu, Chem. Biodivers. 9 (2012) 1533–1544.

[41] A.W. Coats, J.P. Redfern, Nature 20 (1964) 68–79.

[42] H.W. Horowitz, G. Metzger, Anal. Chem., 35 (1963) 1464–1468.

[43] M.M. Omar, G.G. Mohamed, Spectrochim. Acta Part A 61 (2005) 929–936.

[44] A.A. Frost and R.G. Pearson, "Kinetics and Mechanisms", Wiley, New York, 1961.

[45] S.S. Kandil, G.B. El-Hafnawy and E.A. Baker, Thermochim. Acta 414 (2004) 105–113.

[46] N.S. Habib, S.M. Rida, E.A.M. Badawey, H.T.Y. Fahmy, H.A. Ghozlan, Eur. J. Med. Chem. 32 (1997) 759–762.

Table 1. Elemental analyses of Ni(II) complexes (see Fig. 1).

Complexes	Experimental (calculated) (%)				
	C	H	N	S	M
$[Ni(L_1)(CH_3COO)(OH_2)_2]\ H_2O$ **(1)**	32.74 (32.90)	3.31 (3.43)	9.41 (9.60)	14.36 (14.62)	13.38 (13.41)
$[Ni(L_2)(CH_3COO)(OH_2)_2]\ 2H_2O$ **(2)**	32.55 (32.75)	3.23 (3.41)	9.35 (9.55)	14.43 (14.56)	13.67 (13.35)
$[Ni(L_3)(CH_3COO)(OH_2)_2]\ H_2O$ **(3)**	32.25 (32.38)	3.00 (3.19)	10.02 (10.30)	15.54 (15.70)	14.62 (14.40)
$[Ni(L_4)(CH_3COO)(OH_2)_2]\ H_2O$ **(4)**	29.04 (29.16)	2.54 (2.65)	12.19 (12.37)	13.86 (14.14)	12.70 (12.96)

Table 2. Quantum chemical parameters of Ni(II) complexes.

Complex[a]	E_{HOMO} (eV)	E_{LUMO} (eV)	ΔE (eV)	χ (eV)	η (eV)	σ $(eV)^{-1}$	Pi (eV)	S $(eV)^{-1}$	ω (eV)	ΔN_{max}
(1)	-6.086	-4.417	1.669	5.252	0.835	1.198	-5.252	0.599	16.524	6.293
(2)	-6.120	-4.424	1.696	5.272	0.848	1.179	-5.272	0.590	16.388	6.217
(3)	-6.154	-4.440	1.714	5.297	0.857	1.167	-5.297	0.583	16.370	6.181
(4)	-6.665	-4.936	1.729	5.801	0.865	1.157	-5.801	0.578	19.459	6.709

[a]Numbers as given in Table 1

Table 3. Ligand field parameters of the Ni(II) complexes.

Complex[a]	Dq (cm^{-1})	B (cm^{-1})	β	β^o %	Dq/B	LFSE (kcal mol^{-1})
(1)	1328	526	0.507	49.3	2.52	45.64
(3)	1312	131	0.126	87.4	10.02	45.09
(4)	1277	606	0.584	41.6	2.11	43.89

[a]Numbers as given in Table 1

Table 4. Thermal analysis data of the Ni(II) complexes.

Complex[a]	Temp. range (ºC)	Found mass loss (calc.) %	Assignment
(1)	60-96	4.07 (4.11)	Loss of one water molecule in outside of the coordination sphere
	96-408	40.64 (39.07)	Loss of two coordinated water molecules and loss of one coordinated acetate group, further decomposition of a part of the ligand (CS_2)
	408-800	27.17 (28.79)	Decomposition of a part of the ligand ($C_5H_8N_3O$)
	> 800	28.12 (28.03)	4C atoms + NiO
(2)	35-107	8.41 (8.19)	Loss of two water molecules in outside of the coordination sphere.
	107-404	37.32 (38.89)	Loss of two coordinated water molecules and loss of one coordinated acetate group, further decomposition of a part of the ligand (CS_2).
	404-800	30.43 (30.48)	Decomposition of a part of the ligand ($C_7H_8N_3$)
	> 800	23.84 (22.45)	2C atoms + NiO
(3)	45-99	4.81 (4.42)	Loss of one water molecule in outside of the coordination sphere
	99-400	37.43 (37.77)	Loss of two coordinated water molecules and loss of one coordinated acetate group, further of a part of the ligand (CSNH).

	400-800	29.65 (30.66)	Decomposition of a part of the ligand ($C_5H_5N_2S$)
	> 800	28.11 (27.15)	3C atoms + NiO
(4)	45-109	3.24 (3.98)	Loss of one water molecule in outside of the coordination sphere
	109-408	47.18 (46.61)	Loss of two coordinated water molecules and loss of one coordinated acetate group, further of a part of the ligand ($C_2S_2N_2$).
	408-800	25.47 (24.96)	Decomposition of a part of the ligand ($C_4H_5N_2O_2$).
	> 800	24.11 (24.45)	3C atoms + NiO

[a]Numbers as given in Table 1

Table 5. Thermodynamic data of the thermal decomposition of Ni(II) complexes.

Complex[a]	Decomposition temperature (^oC)	Method	Parameter					Correlation coefficient (r)
			E_a (kJ mol^{-1})	A (s^{-1})	ΔS^* (J mol^{-1} K^{-1})	ΔH^* (kJ mol^{-1})	ΔG^* (kJ mol^{-1})	
(1)	150-400	CR	39.9	8.56×10^{0}	-232	35.3	163	0.99707
		HM	49.7	3.17×10^{2}	-202	45.9	157	0.99761
	400-555	CR	131	4.29×10^{6}	-126	125	220	0.99681
		HM	145	9.83×10^{7}	-99.6	139	214	0.99850
(2)	158-395	CR	43.2	1.91×10^{1}	-225	38.6	163	0.99817
		HM	53.1	5.87×10^{2}	-197	48.6	157	0.99195
	395-533	CR	88.8	3.14×10^{3}	-186	82.6	219	0.99872
		HM	99.4	6.04×10^{4}	-161	93.2	212	0.99931
(3)	145-400	CR	38.7	5.54×10^{00}	-236	34.2	163	0.99771
		HM	49.5	2.61×10^{2}	-204	45.0	157	0.99361
	400-535	CR	101	2.38×10^{4}	-169	94.8	220	0.99784
		HM	114	6.93×10^{5}	-141	108	212	0.99800
(4)	160-410	CR	58.1	4.36×10^{2}	-200	53.4	165	0.99723
		HM	68.4	1.67×10^{4}	-169	63.8	158	0.99580
	410-550	CR	118	3.80×10^{5}	-146	111	221	0.99557

		HM	131	8.06×10^{6}	-120	124	215	0.99841

[a]Numbers as given in Table 1

Table 6. Antibacterial activity data of Ni(II) complexes and standard drug. The results were recorded as the average diameter of inhibition zone (mm) ± standard deviation.

Compound[a]	Conc. (µg/mL)	Gram positive bacteria		Gram negative bacteria	
		Bacillus cereus	*Staphylococcus aureus*	*Escherichia coli*	*Klebsiella pneumoniae*
(1)	50	-ve	-ve	-ve	2 ± 0 *
	100	-ve	-ve	-ve	2 ± 0.14 *
	150	-ve	-ve	-ve	3 ± 0.28 *
(2)	50	1 ± 0	-ve	-ve	2 ± 0.14 *
	100	1 ± 0.14	-ve	-ve	3 ± 0 *
	150	1 ± 0	1 ± 0	-ve	3 ± 0.14 *
(3)	50	-ve	-ve	1 ± 0	2 ± 0.28 *
	100	-ve	-ve	1 ± 0	2 ± 0.14 *
	150	-ve	-ve	1 ± 0	3 ± 0 *
(4)	50	1 ± 0	-ve	-ve	2 ± 0.14 *
	100	-ve	-ve	-ve	2.025 ± 0.035 *
	150	-ve	-ve	-ve	2 ± 0.14 *
Penicillin	50	1 ± 0.14	2 ± 0	1 ± 0	-ve
	100	3 ± 0.28	2 ± 0.14	3 ± 0	-ve
	150	3 ± 0.14	2 ± 0	3 ± 0	-ve

[a]Numbers as given in Table 1.

* Indicate significant different value from that of penicillin.

Table 7. Antifungal activity data of Ni(II) complexes and standard drug. The results were recorded as the average diameter of inhibition zone (mm) ± standard deviation

Compound[a]	Conc. (µg/mL)	*Aspergillus niger*	*Fusarium oxysporum*	*Alternaria alternata*	*Penicillium italicum*
(1)	50	-ve	-ve	-ve	5 ± 0 *
	100	-ve	-ve	-ve	6 ± 0.14 *
	150	-ve	-ve	-ve	2 ± 0
(2)	50	-ve	-ve	-ve	-ve
	100	-ve	-ve	-ve	2 ± 0
	150	2 ± 0.14	-ve	-ve	-ve
(3)	50	1 ± 0	-ve	-ve	-ve
	100	2 ± 0.14	-ve	-ve	5 ± 0.28
	150	2 ± 0.14	-ve	-ve	5 ± 0.14
(4)	50	1 ± 0	-ve	-ve	-ve
	100	1 ± 0	-ve	-ve	-ve
	150	2 ± 0.14	-ve	-ve	-ve
Miconazole	50	1 ± 0	2 ± 0	5 ± 0	1 ± 0
	100	3 ± 0.14	3 ± 0	6 ± 0	1 ± 0

	150	4 ± 0	3 ± 0	6 ± 0.14	2 ± 0

[a]Numbers as given in Table 1.

* Indicate significant different value from that of miconazole.

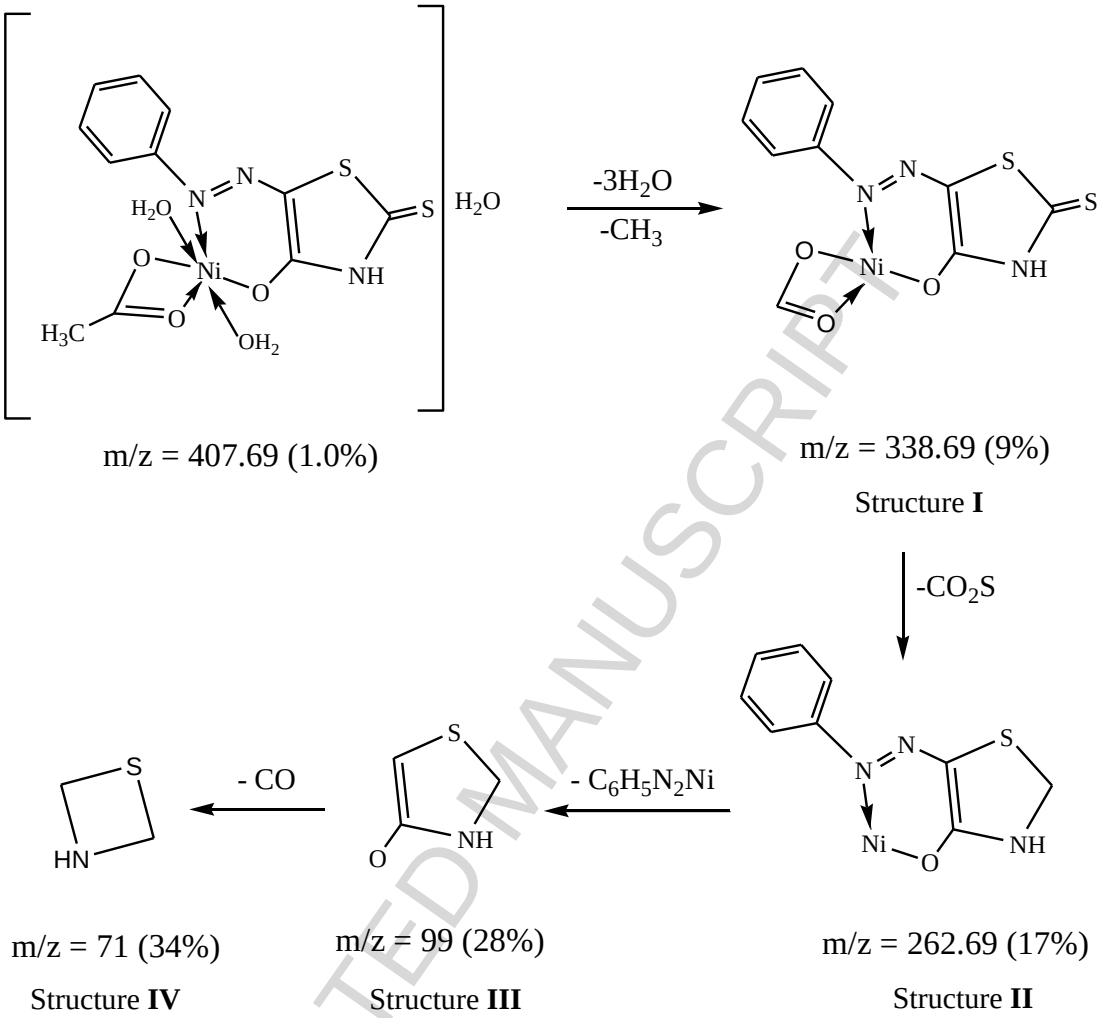

Scheme 1. Fragmentation patterns of complex **(3)**.

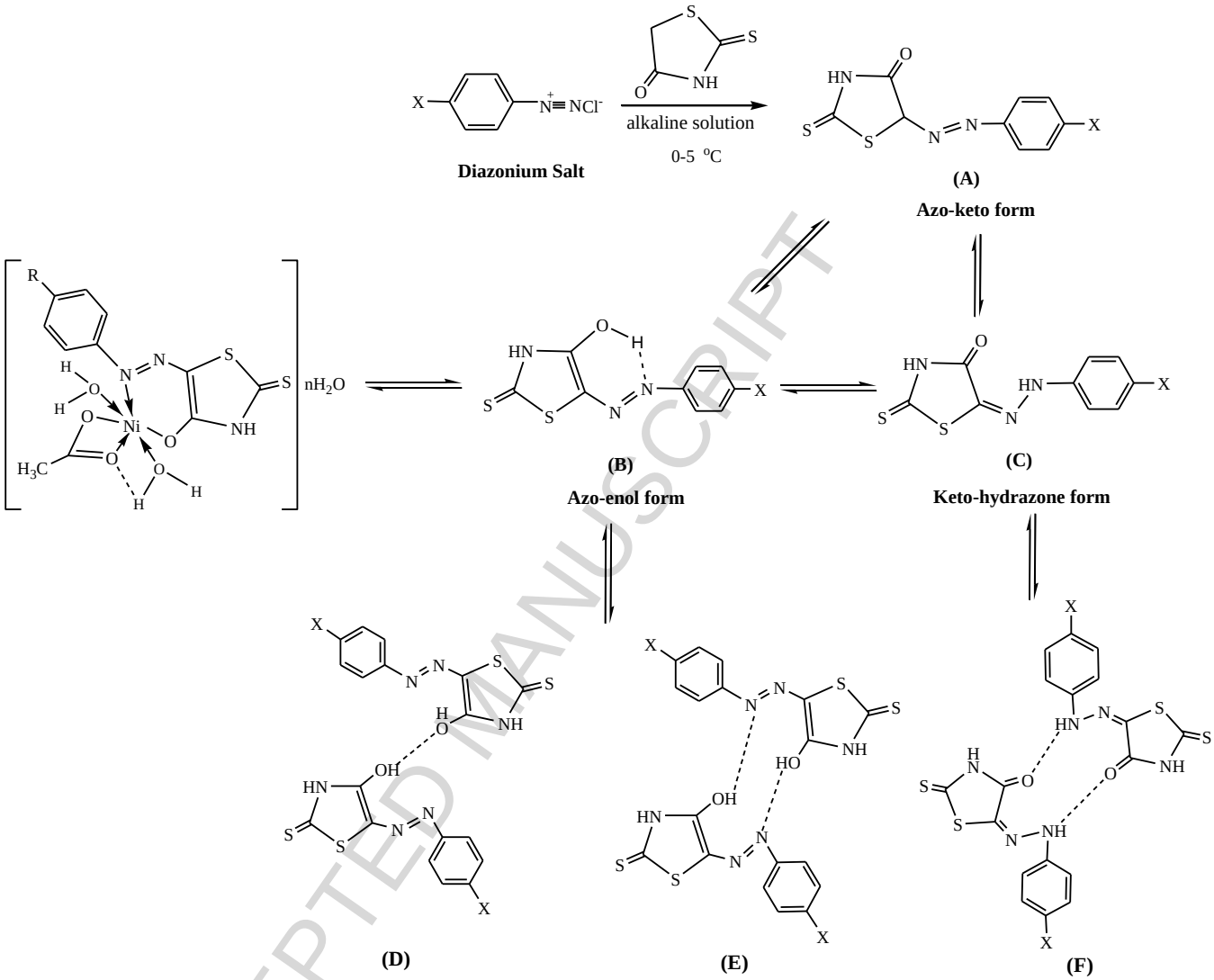

n=1, R = OCH_3 (HL_1); n=2, CH_3 (HL_2); n=3, H (HL_3) and n=4, NO_2 (HL_4)

Fig. 1. Structure of intramolecular and intermolecular hydrogen bonds of azo dye ligands and their Ni(II) complexes.

	HOMO	LUMO
Complex **(1)**	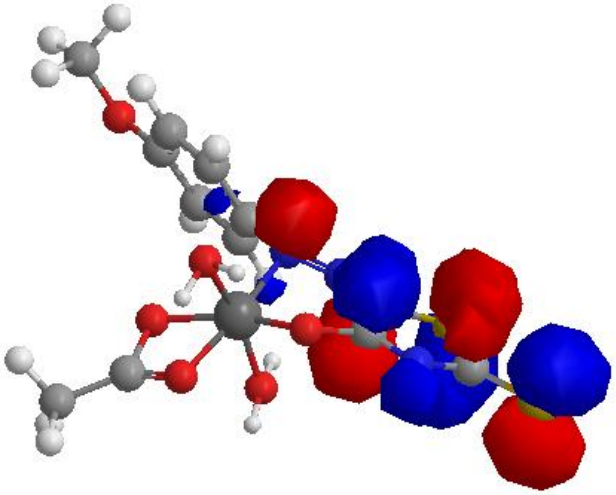	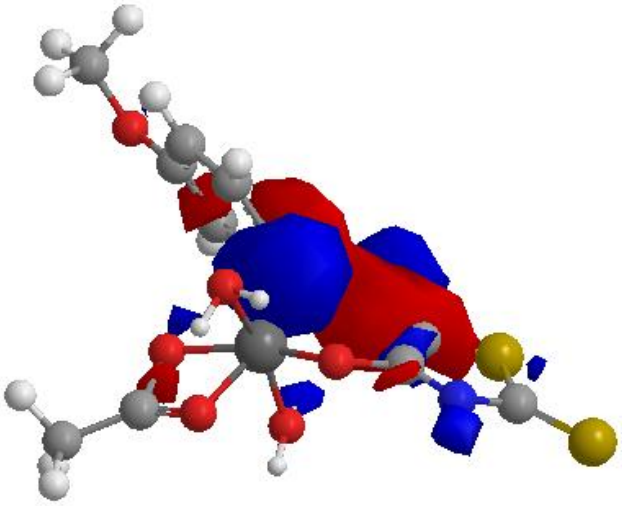
Complex **(2)**	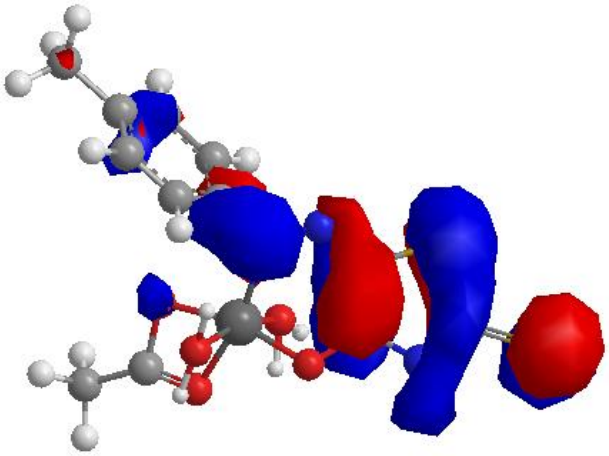	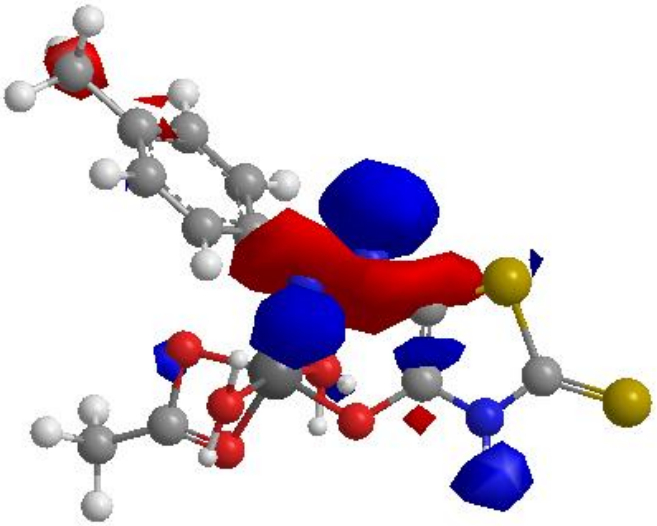
Complex **(3)**	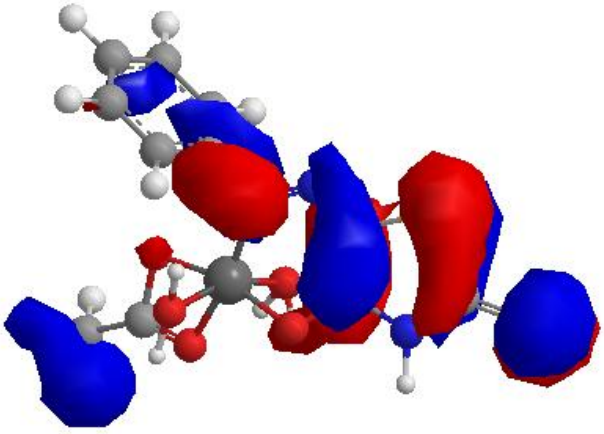	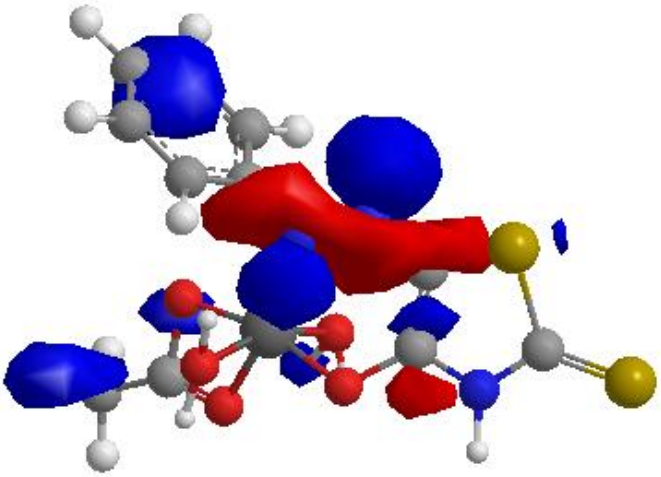

Complex **(4)**

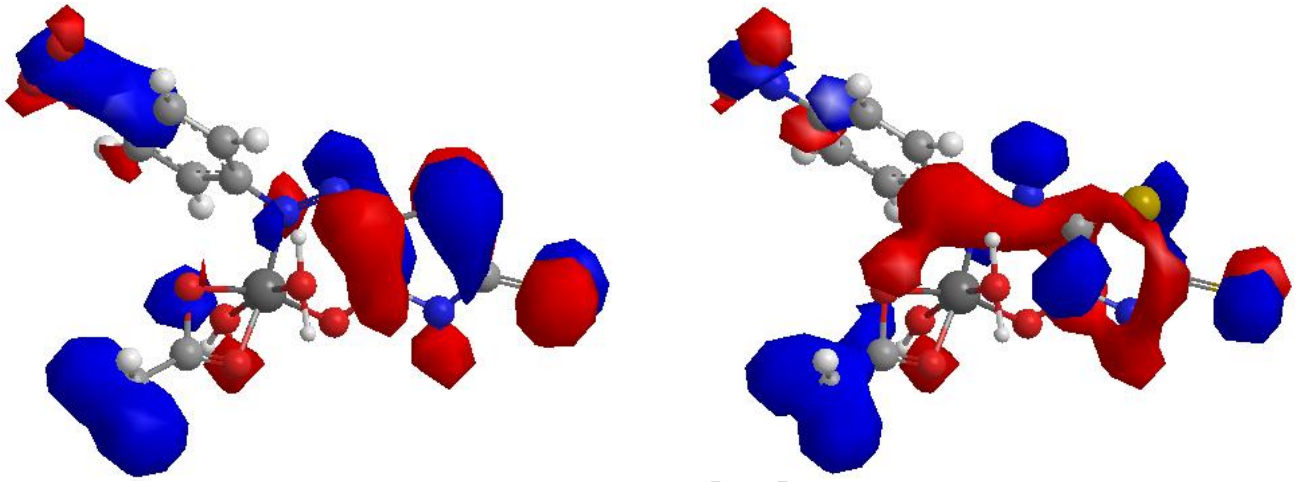

Fig. 2. Molecular structures (HOMO & LUMO) of Ni(II) complexes.

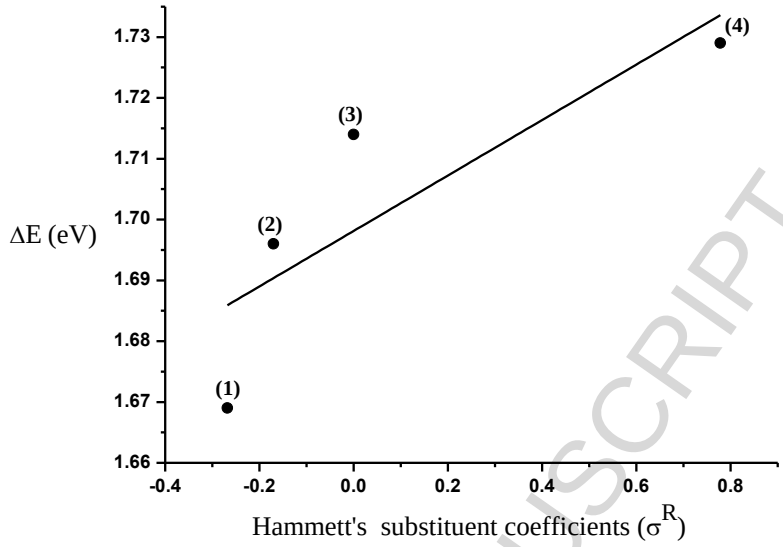

Fig. 3. The relation between Hammett's substituent coefficients (σ^R) *vs*. HOMO–LUMO energy gap (ΔE) of Ni(II) complexes.

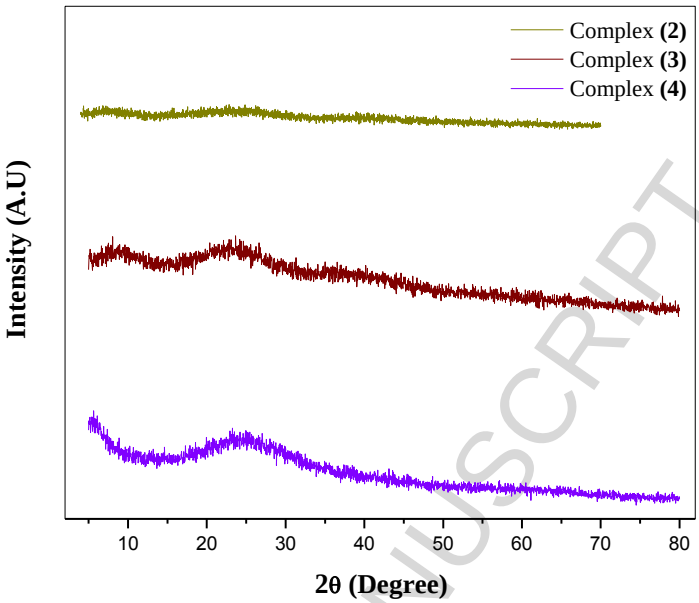

Fig. 4. X-ray diffraction patterns of powder forms for Ni(II) complexes.

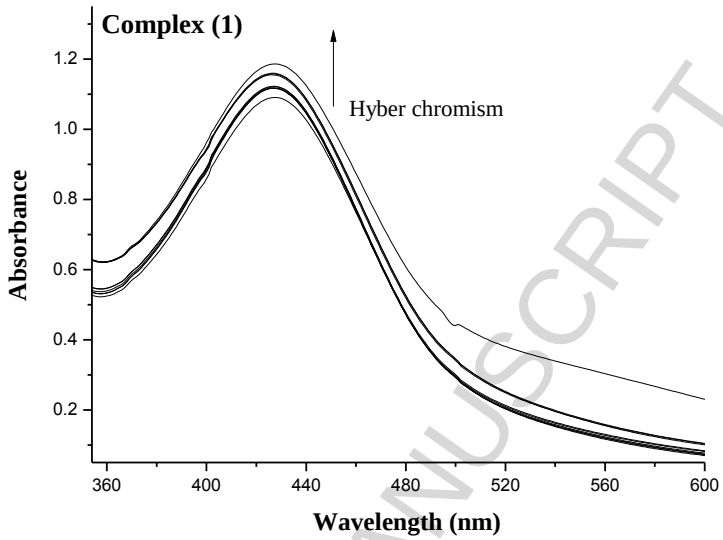

Fig. 5. Absorption spectrum of Ni(II) complex **(1)** in buffer pH 7.2 in the presence of increasing amount of CT-DNA. Arrows indicate the changes in absorbance upon increasing the CT-DNA concentration.

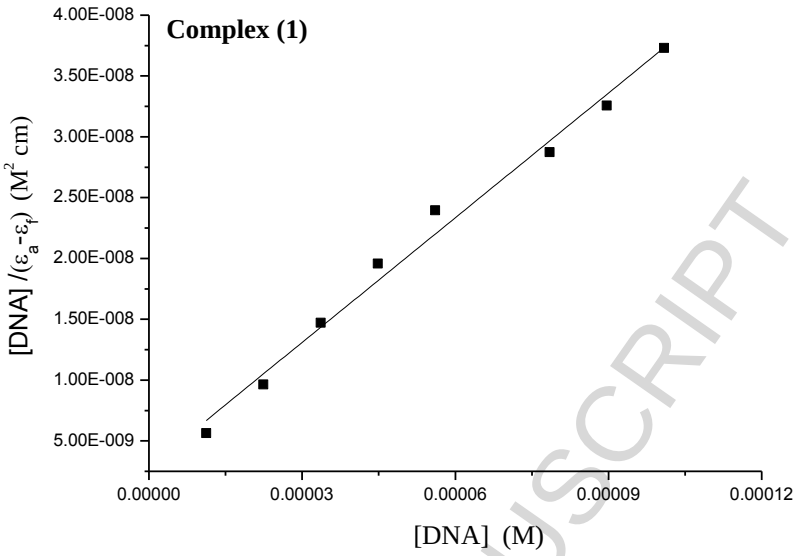

Fig. 6. Plot of $[DNA]/(\varepsilon_a - \varepsilon_f)$ (M^2 cm) *vs.* [DNA] (M) for titration of DNA with Ni(II) complex **(1)**.

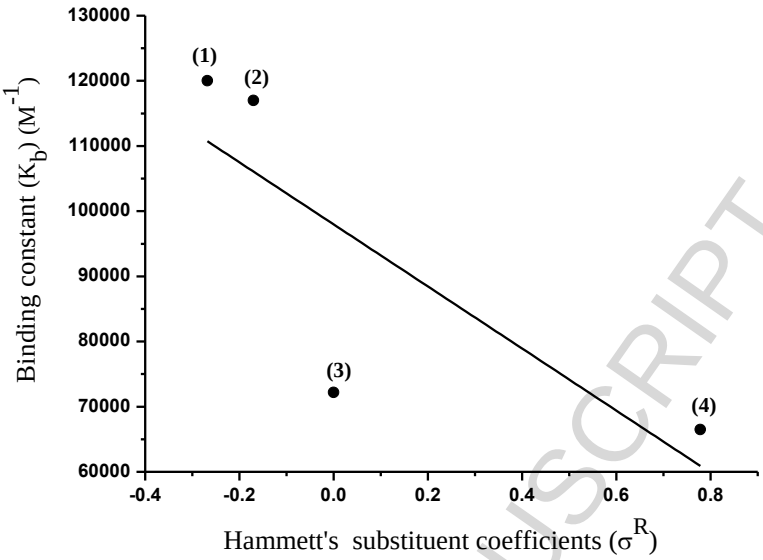

Fig. 7. The relation between Hammett's substituent coefficients (σ^R) *vs.* binding constants (K_b) of Ni(II) complexes.

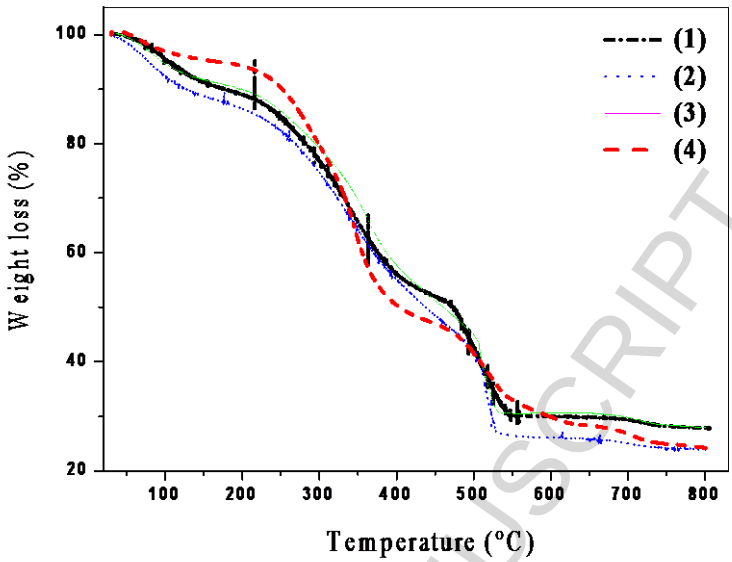

Fig. 8. TGA curves for Ni(II) complexes.

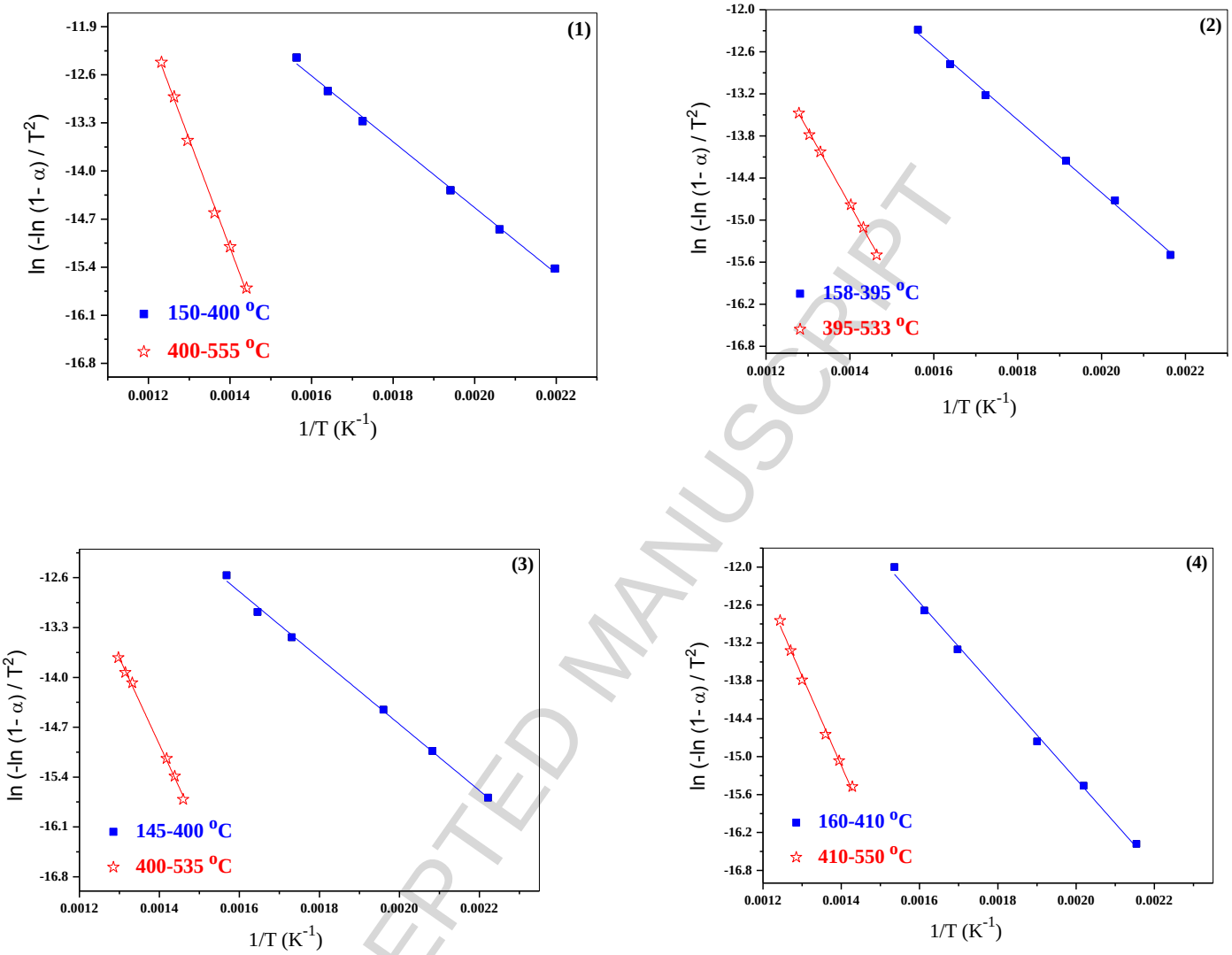

Fig. 9. Coats–Redfern (CR) of the Ni(II) complexes.

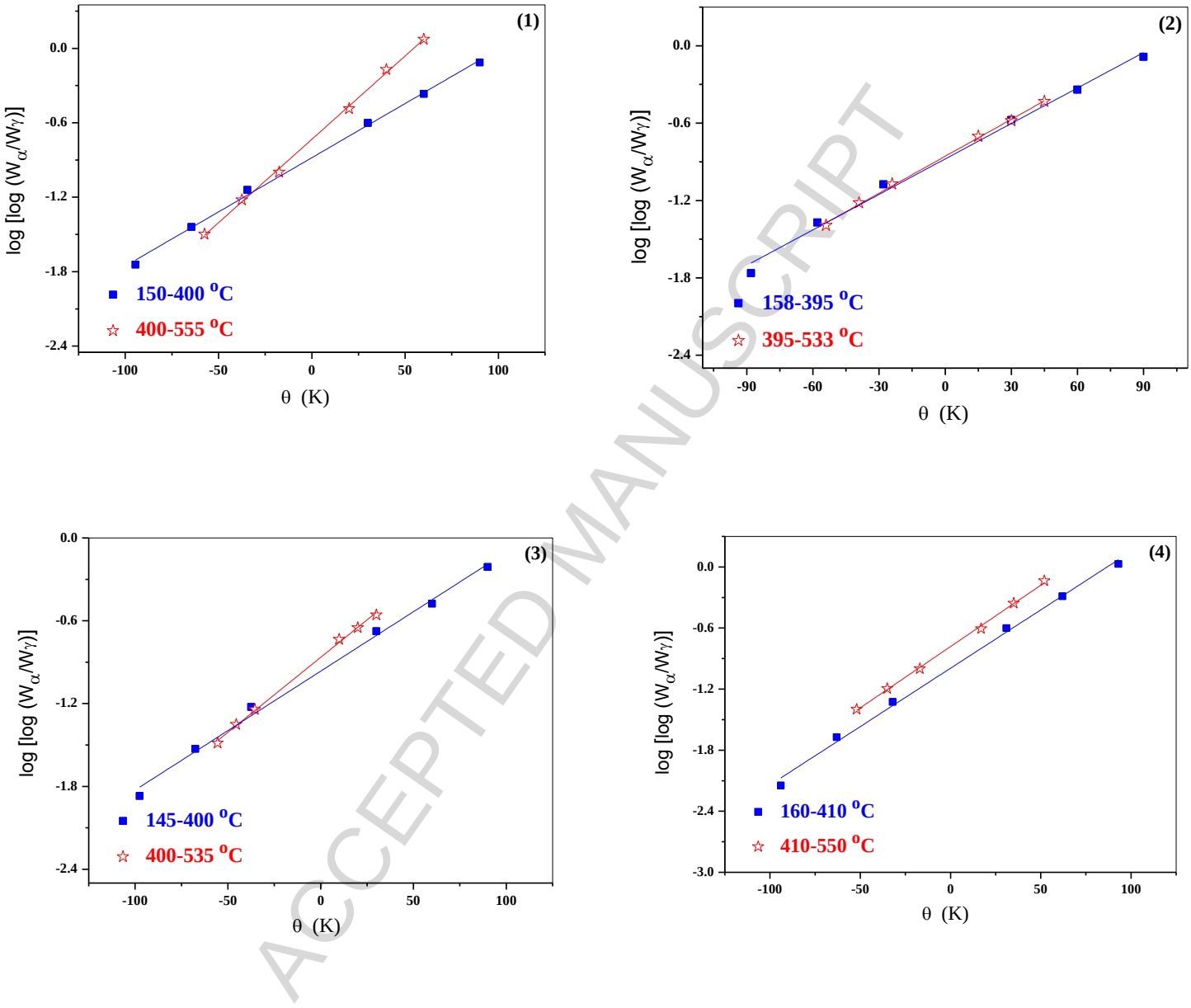

Fig. 10. Horowitz-Metzger (HM) of the Ni(II) complexes.

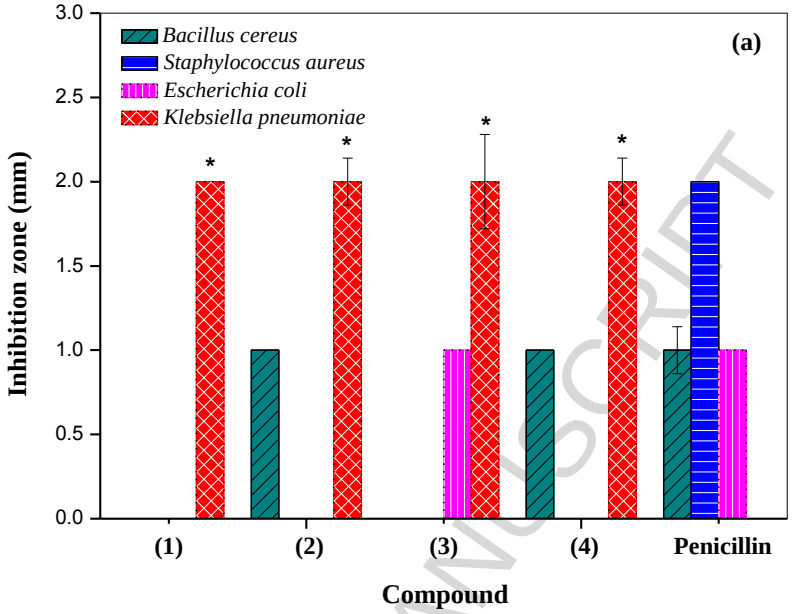

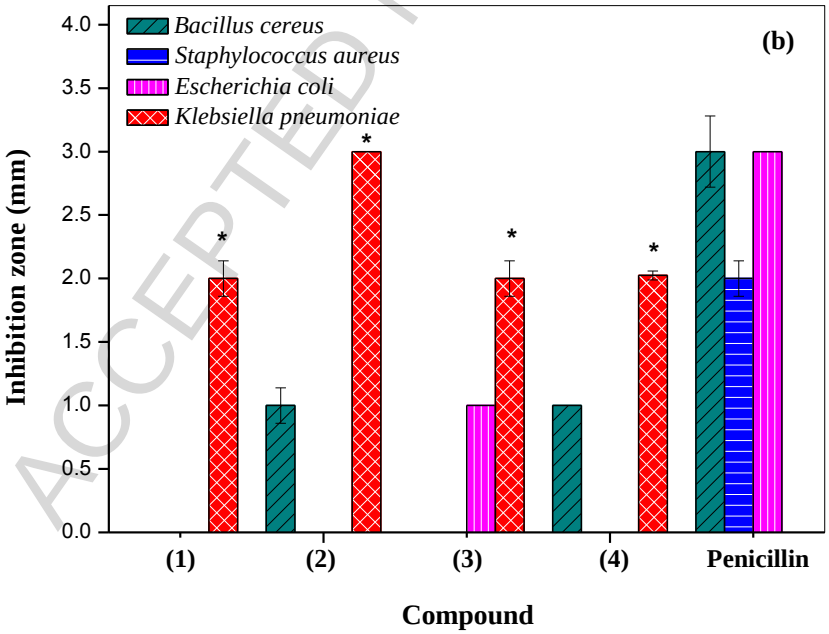

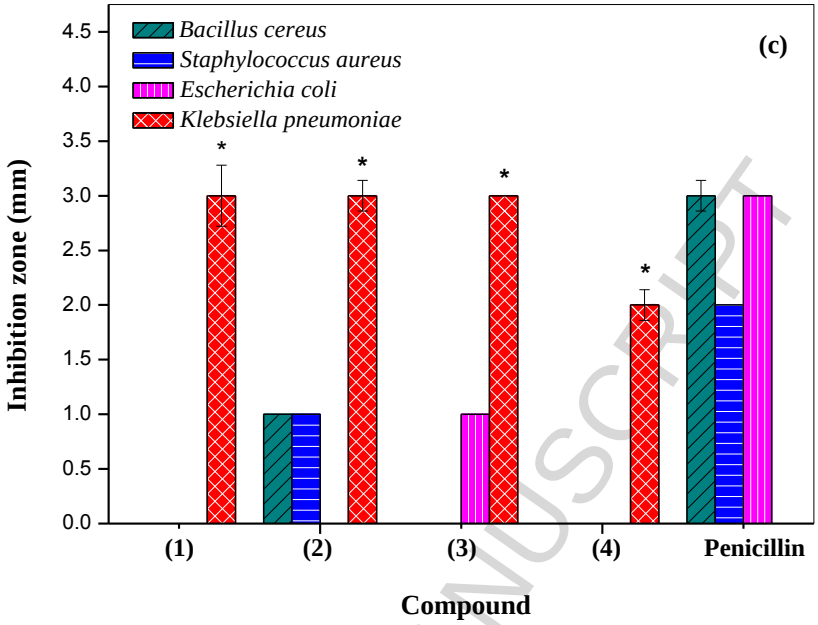

Fig. 11. Antibacterial activity data of Ni(II) complexes and standard drug at tested concentrations a) 50, b) 100 and c) 150 µg/mL. Inhibition zone was recorded as mm.

* Indicate significant different value from that of penicillin.

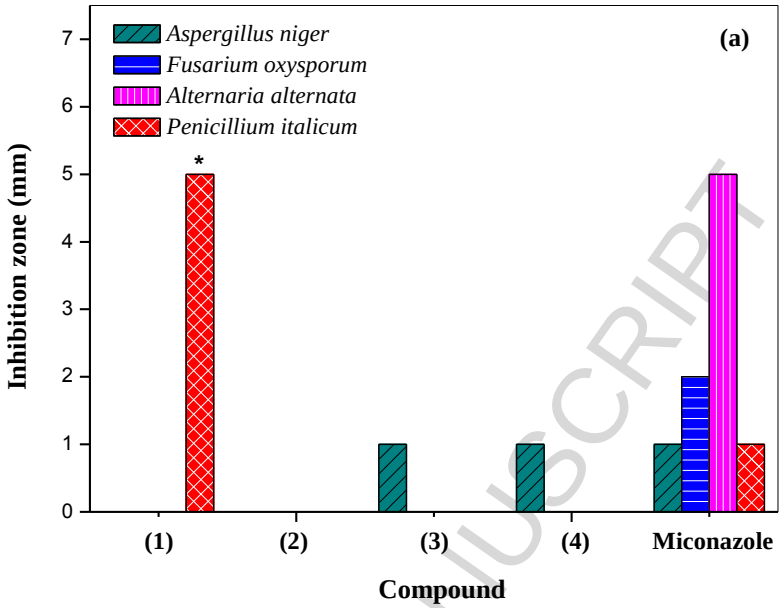

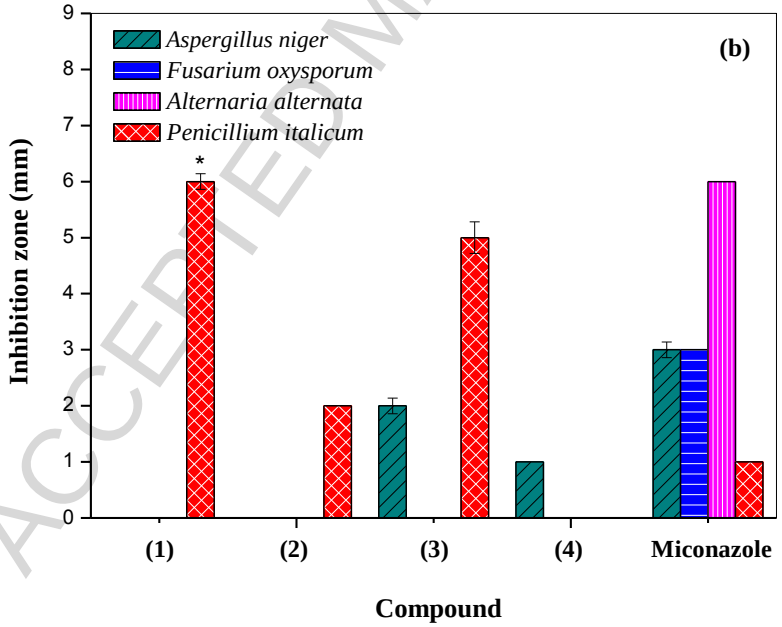

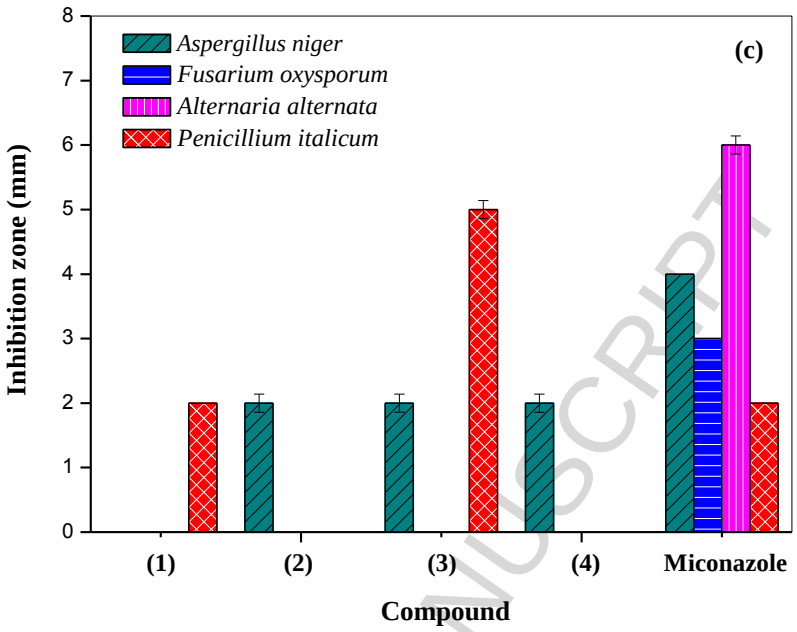

Fig. 12. Antifungal activity data of Ni(II) complexes and standard drug at tested concentrations a) 50, b) 100 and c) 150 µg/mL. Inhibition zone was recorded as mm.

* indicate significant different value from that of miconazole.

The relation between Hammett's substituent coefficients (σ^R) *vs.* binding constants (K_b) of Ni(II) complexes **(1-4)**.

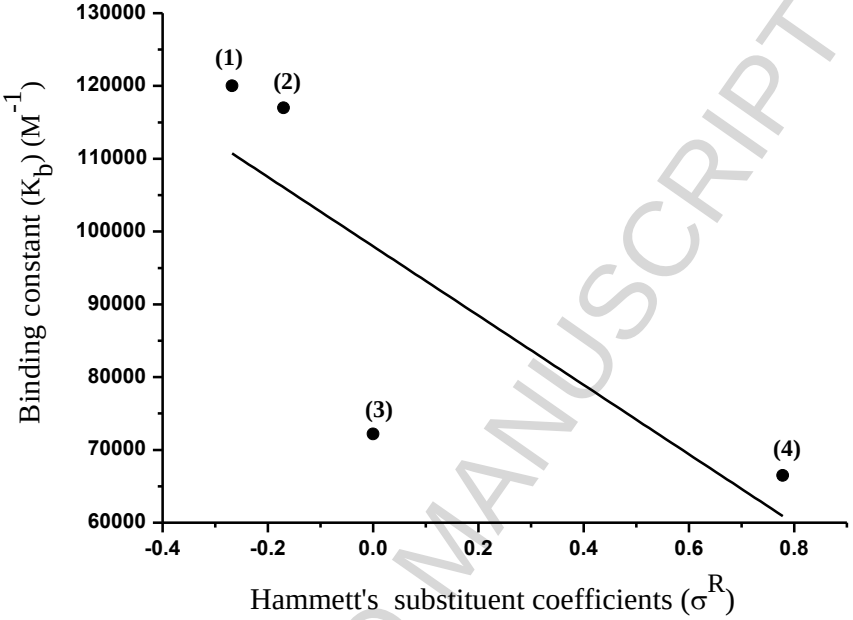

Graphical abstract

Highlights

- Ni(II) complexes of rhodanine azo dye derivatives are prepared and characterized
- The antibacterial and antifungal activities of Ni(II) complexes are investigated
- The interaction between Ni(II) complexes and calf thymus DNA (CT-DNA) shows hyperchromism effect
- The thermodynamic parameters of Ni(II) complexes are calculated and discussed